Author manuscript, published in "The 2013 Computing in Cardiology Conference (2013)"

hal-00850363, version 1 - 5 Sep 2013

Experimental study of arrhythmia due to mild therapeutic hypothermia after resuscitation of cardiac arrest

B. Xu[1], O. Pont[1], G. Laurent[2], S. Jacquir[2], S. Binczak[2], H. Yahia[1]
[1]Géostat, INRIA Bordeaux Sud-Ouest, 33405 Talence, France
[2]CNRS UMR 5158 Dijon France, LE2I Université de Bourgogne, Dijon France

Abstract

The therapeutic hypothermia (under $34\,^{\circ}\mathrm{C} - 32\,^{\circ}\mathrm{C}$ *during* $12 - 24h$*) can help reduce cerebral oxygen demand and improve neurological outcomes after the cardiac arrest. However it can have many adverse effects. The cardiac arrhythmia generation represents an important part among these adverse effects. In order to study the arrhythmia generation after therapeutic hypothermia, an experimental cardiomyocytes model is used. The experiments showed that at* $35\,^{\circ}\mathrm{C}$*, the acquired extracellular potential of the culture are characterized by period-doubling phenomenon. Spiral waves are observed as well in this case. The results suggested that the global dynamics of therapeutic hypothermia after cardiac arrest can be represented by a Pitchfork bifurcation, which could explain the different ratio of arrhythmia among the adverse effects after this therapy. A variable speed of cooling / rewarming, especially when passing* $35\,^{\circ}\mathrm{C}$*, would help reduce the post-hypothermia arrhythmia.*

1. Introduction

One of the important challenges after cardiac arrest (CA) is the neurological damage of the brain. In case of resuscitation after CA, the brain suffers the ischemia and the inflammation from reperfusion [1]. Currently, the only therapy available is the mild therapeutic hypothermia (MTH) : put the patient under $34\,^{\circ}\mathrm{C} \sim 32\,^{\circ}\mathrm{C}$ during $12 - 24$ hours [2–4]. In fact, the use of therapeutic hypothermia following cardiac arrest was reported in the late 1950s [5, 6]. The results showed some benefits but uncertain. It was also clinically difficult to control the interval between arrest and cooling which is very important. Therefore, hypothermia for cardiac arrest has waned for years. Over the past few years, the therapeutic hypothermia began to redraw attentions of researchers, clinicians etc.. In 2003, The American Heart Association (AHA) endorsed the use of therapeutic hypothermia following cardiac arrest. Even though that MTH has been shown to increase the hospital survival rate, it has many adverse effects, among which the cardiac arrhythmia generation represents an important part (up to 34%) [7, 8]. Cardiac culture in vitro provides a better spatial resolution (down to cellular level) than studies in vivo, which could bring some insights of the mechanism of post-hypothermia arrhythmia (PHA) generation.

2. Materials and Methods

Monolayer cardiac culture is prepared with cardiomyocytes (CM) from new-born rat ($1 \sim 4$ days) directly on a multi-electrodes array (MEA), a system allowing real-time recording the extracellular field potential (EFP) of the CM culture, (details of culture preparing in [9]). The CM cultures have the potential to reproduce in vitro a wide range of pathological conditions such as ischemia reperfusion, the radical stress or thermal shock, and any combination of these conditions [9]. The EFP signals correspond to the combination of 1^{st} or 2^{nd} order derivatives of action potential (AP). Their peaks corresponds to AP depolarization (Figure 1, *Right*). This relationship allows to interpreting indirectly the results at "action potential propagation" level.

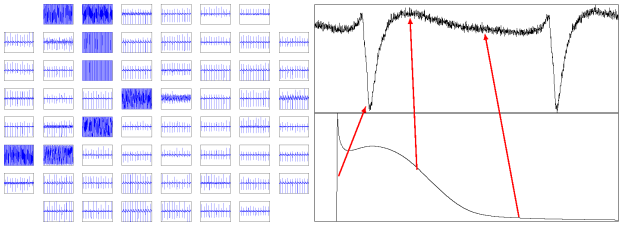

Figure 1: *Left* :EFP in basal conditions. Every panel corresponding to an acquisition, placed according to their position on the MEA. *Right* : relationship between the EFP and the action potential.

The acquired signals are then analyzed with two methods from nonlinear dynamics theory : phase space reconstruction and detrended fluctuation analysis.

Phase space reconstruction The basic principle of method phase space reconstruction is to map the dynamical evolution of a time series into a geometrical object

hal-00850363, version 1 - 5 Sep 2013

embedded in an abstract representation space. This object represents all possible internal states (phases) of the system that produced the time series. Furthermore, each dynamical state corresponds to a unique point, so that the reconstructed space shares the same topological properties as the original phase space of the system dynamics [10]. Mathematically, under the approach phase space reconstruction, the system can be represented as :

$$\vec{X}(\tau, m) = [x(t), x(t+\tau), \ldots, x(t+\tau(m-1))], \quad (1)$$

where $\vec{X}$ denotes the system states and is a function of τ and m, $x(t)$ is the time series ($t = 0, 1, 2, \ldots$), m is the embedding dimension and τ is the time lag. m is estimated by the method False Nearest Neighbor (FNN) [11], which intends to find the minimal embedding dimension. As for time lag τ, a method based on autocorrelation function is used to find optimal values (largest one so that the resulting coordinates for m are relatively independent) [12].

Detrended fluctuation analysis Detrended fluctuation analysis is a method for determining the statistical self-affinity of a signal. It unmasks long-memory processes (revealing the extent of long-range correlations) in time series [13]. It is more robust and less prone to artefacts than a simple period analysis. A time series $x(t)$ has N samples. It is firstly integrated, then the obtained new time series $y(t)$ is divided into boxes of equal length n. A least squares line is performed for every detrended signal of length n in order to fit to the data. The y coordinate of the straight line segments is denoted by $y_n(t)$, the local trend. Next, the integrated time series $y(t)$ is detrended by subtracting $y_n(t)$, in each box. The root-mean-square fluctuation of this integrated and detrended time series is calculated by

$$F(n) = \left[\frac{1}{N} \sum_{t=1}^{N} [y(t) - y_n(t)]^2 \right]^{\frac{1}{2}} \propto n^{\alpha}. \quad (2)$$

This computation is repeated over all time scales (box sizes) to characterize the relationship between $F(n)$, the average fluctuation, and the box size, n. Using log-log plot, a linear relationship would indicates the presence of power law (fractal) scaling, where the fluctuations can be characterized by the slope of the line relating $\log F(n)$ to $\log n$. In other words, this scaling exponent α captures the dynamical complexity of activation signals.

3. Results

In order to simulate the MTH conditions, the experiments consist of two parts : culture cooling (37 °C → 30 °C) and re-warming (30 °C → 37 °C). Typical EFP signals can be found in Figure 2. When the temperature of the culture is decreasing, the periods of EFP signals increase in general (Figure 2 *Right*). Apart from T ≠ 35 °C, their periods are relatively stable. The slight variation of these periods could be the consequence of junction-gap remodeling [14]. From 37 °C to 30 °C, the period is increased from about 0.5 s to 1.58 s. Two period values are shown at 35 °C : the lower value is almost exactly the same as the one at 37 °C, higher value is roughly the double (Figure 2 *Right*). From a point view of nonlinear dynamics, this period-doubling is a marker when a system is conducted to stat “chaos” [15].

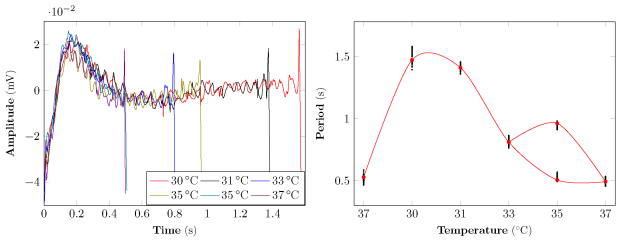

Figure 2: *Left* : comparison of typical single period EFP signals at different temperatures. *Right* : periods digram, periods-doubling at T = 35 °C, black points are periods values, red ones are median vales of periods at corresponding temperature.

These signals can be also reconstructed as an activation map, which gives a tow-dimensional view of the signals dynamics in the culture. When T ≠ 35 °C, the dynamics of the signals is in form of plane wave propagation (Figure 3). At 35 °C, spiral waves are observed in the activation map which is commonly considered as a sign of cardiac arrhythmia (Figure 4).

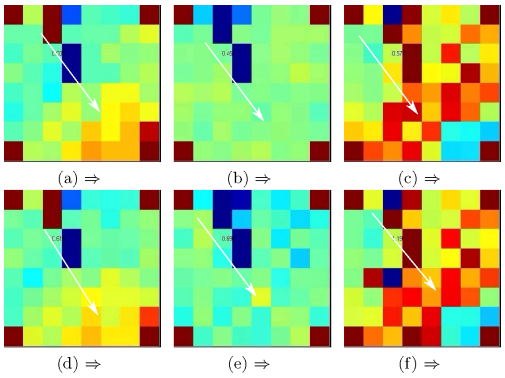

Figure 3: Plane wave propagation when T ≠ 35 °C, from time (a) to (f). White arrows indicate the propagation direction of plane wave

From the reconstructed phase space, doubling-trajectories and rare tripling-trajectories are found. It implies that the general dynamics of MTH could be presented as a pitchfork bifurcation, which could explain exactly the doubling-trajectories and tripling-trajectories phenomena. These re-

hal-00850363, version 1 - 5 Sep 2013

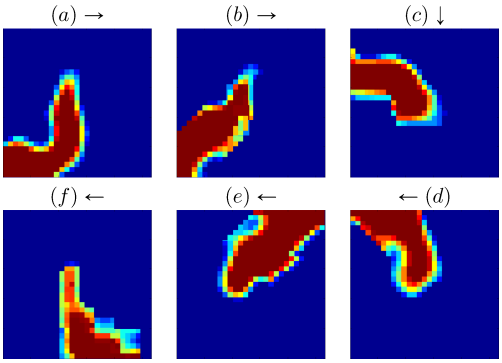

Figure 4: Spiral wave propagation with clockwise rotation at $\mathrm{T} = 35\,^{\circ}\mathrm{C}$, from time (a) to (f). *images filtered from the original ones in order to better represent the spiral wave*

sults at cellular level agreed with other clinical studies on MTH.

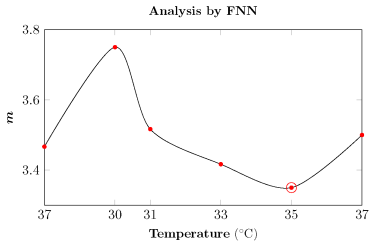

Figure 5: mean embedding dimension m vs. temperature

As shown in Figure 5, the mean embedding dimension m initially decreases when temperature drops from 37 °C to 35 °C. It increases then slowly up to 3.52 at 31 °C to another transition point. The m increases abruptly after 31 °C. When rewarming, the temperature returns to 37 °C and m recovers its original value. This reinforces the evidence that a temperature around 35 °C contains a transition point for the system. With the method DFA, a similar result (**??**) could be obtained : Here, bimodality occurs at

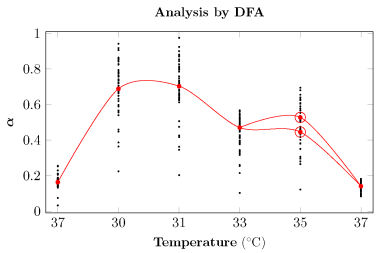

Figure 6: Detrended fluctuation analysis. α vs. temperature. Black points are α values, red ones are main median vales of α at corresponding temperature

$\mathrm{T} \approx 35\,^{\circ}\mathrm{C}$ again, further confirming it as a transition point.

Attractors of trajectories in reconstructed phase spaces at different temperatures are presented in the following Figure 7 : The trajectories in phase space have all been

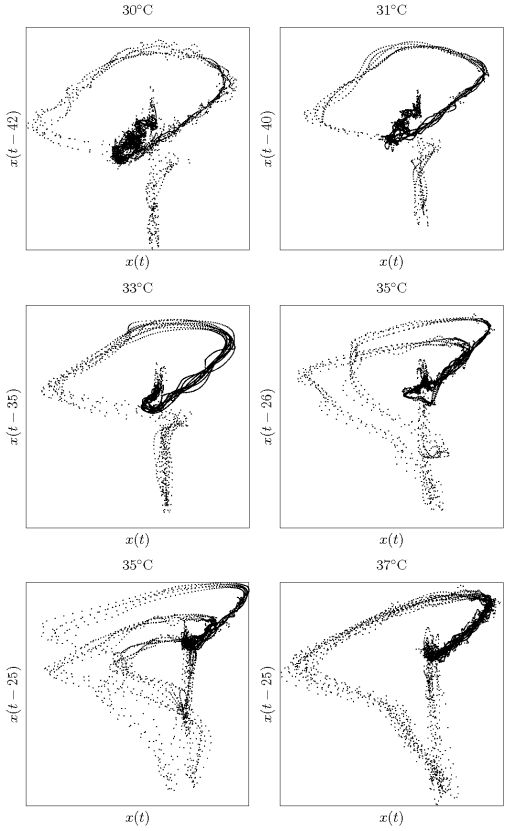

Figure 7: Phase space reconstruction for typical signals at different temperatures. Bifurcation / trifurcation at $\mathrm{T} \approx 35\,^{\circ}\mathrm{C}$. *time lagging unit: samples*

well-formed. Apart from 35 °C, though the original signals are different, the global forms of the attractors are similar with a little variation.

Bifurcation at $\mathrm{T} \approx 35\,^{\circ}\mathrm{C}$ also reveals in attractors themselves. Even a rare trifurcation is found. Here arises a hypothesis : the phase transition consistent with a supercritical pitchfork bifurcation. The process could be represented as in Figure 8. The bold black line denotes the stable states of the system. In the dashed line, the system is in an unstable dynamic state, but it could sustainedly remain there if quasistatic perturbations are not strong enough to make it fall to the (dynamical) lower energy states. This makes that state a metastable state. From $\mathrm{T} = 35\,^{\circ}\mathrm{C}$, the system enters the unstable region. For example, if the system follows the blue trajectory, it will cross twice stability line, which makes the period-doubling and so bifurcation in phase space will occur. If the system follows the red trajectory, it will cross the stability line three times and exhibit trifurcation. Since in this region the transition between stable and unstable states is fast and in most cases it

hal-00850363, version 1 - 5 Sep 2013

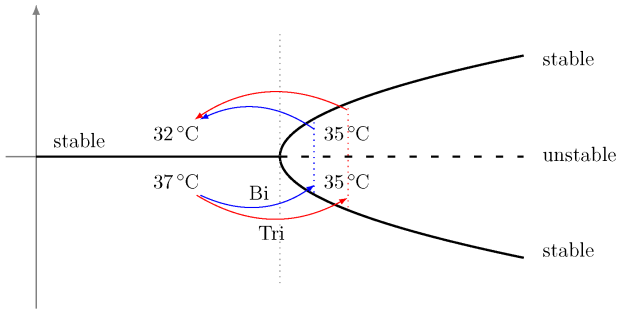

Figure 8: Illustration of Bifurcation or Trifurcation (type Pitchfork) of hypothermia effect on EP.

is the unstable states which dominate the system dynamics, the metastable line is not always observed in practice.

4. Conclusions

In this study, the problem of arrhythmia generation after MTH is studied with an experimental cardiomyocytes model. Here, results in vitro confirmed that arrhythmic phenomena happened around 35 °C, which agreed with clinical observations. In clinical trials, it is shown that protective hypothermia effects (below 35 °C) mitigate cardiac arrest. It needs also to remain above 32 °C: threshold of moderate hypothermia, leading to increased risk of organ failure. The results suggested also that the whole process of MTH consistents with supercritical pitchfork bifurcation, with the attractor dimension as order parameter. This hypothesis can well explain the bifurcation phenomena observed in phase space. Depending the path that this process passes, the system can show either bifurcation of trajectories or trifurcation in rarer case. According to the pitchfork bifurcation hypothesis, if the system follows the metastable paths, it could thus avoid arrhythmogenesis. Which means, the post-hypothermia arrhythmia could be avoided.

In practical hypothermia therapy, the cooling or rewarming is often under constant speed, the pitchfork bifurcation hypothesis suggests that a variable speed would help to reduce the rate of post-hypothermia arrhythmia. However, with a faster speed passing 35 °C or a slower speed, it is still unclear. This needs a further study, which is one of the objectives of an on-going project.

Acknowledgements

We acknowledge the Institute of Cardiovascular Research (Dijon, France) and the NVH Medicinal (Dr. David VANDROUX, Dijon, France) for our collaboration in the experimental data acquisition.

References

[1] de Vreede-Swagemakers JJ, Gorgels AP, Dubois-Arbouw WI, van Ree JW, Daemen MJ, et al. (1997) Out-of-hospital cardiac arrest in the 1990s: A population-based study in the maastricht area on incidence, characteristics and survival. Journal of the American College of Cardiology 30: 1500–1505.

[2] Yanagawa Y, Ishihara S, Norio H, Takino M, Kawakami M, et al. (1998) Preliminary clinical outcome study of mild resuscitative hypothermia after out-of-hospital cardiopulmonary arrest. Resuscitation 39: 61–66.

[3] Bernard SA, Gray TW, Buist MD, Jones BM, Silvester W, et al. (2002) Treatment of comatose survivors of out-of-hospital cardiac arrest with induced hypothermia. New England Journal of Medicine 346: 557–563.

[4] Group W, Nolan J, Morley P, al (2003) Therapeutic hypothermia after cardiac arrest: An advisory statement by the advanced life support task force of the international liaison committee on resuscitation. Circulation 108: 118–121.

[5] Williams GR, Spencer FC (1958) The clinical use of hypothermia following cardiac arrest. Annals of Surgery 148: 462–466.

[6] Benson DW, Williams GR, Spencer FC, Yates AJ (1959) The use of hypothermia after cardiac arrest. Anesthesia & Analgesia 38: 423–428.

[7] Nielsen N, Hovdenes J, Nilsson F, Rubertsson S, et al (2009) Outcome, timing and adverse events in therapeutic hypothermia after out-of-hospital cardiac arrest. Acta Anaesthesiologica Scandinavica 53: 926–934.

[8] HACA (2002) Mild therapeutic hypothermia to improve the neurologic outcome after cardiac arrest. New England Journal of Medicine 346: 549-556.

[9] Athias P, Vandroux D, Tissier C, Rochette L (2006) Development of cardiac physiopathological models from cultured cardiomyocytes. Annales de Cardiologie et d'Angéiologie 55: 90–99.

[10] Takens F (1981) Detecting strange attractors in turbulence. In: Rand D, Young LS, editors, Dynamical Systems and Turbulence, Lecture Notes in Mathematics, Springer Berlin / Heidelberg, volume 898. pp. 366–381.

[11] Kennel MB, Brown R, Abarbanel HDI (1992) Determining embedding dimension for phase-space reconstruction using a geometrical construction. Phys Rev A 45: 3403–3411.

[12] Albano AM, Muench J, Schwartz C, Mees AI, Rapp PE (1988) Singular-value decomposition and the grassberger-procaccia algorithm. Phys Rev A 38: 3017–3026.

[13] Kantelhardt JW, Zschiegner SA, Koscielny-Bunde E, Havlin S, Bunde A, et al. (2002) Multifractal detrended fluctuation analysis of nonstationary time series. Physica A: Statistical Mechanics and its Applications 316: 87–114.

[14] Rohr S (2004) Role of gap junctions in the propagation of the cardiac action potential. Cardiovascular Research 62: 309–322.

[15] Ho-Kim Q, Kumar N, Kumar N, Lam H (2004) Invitation to Contemporary Physics. World Scientific.